Bulgarian Chemical Communications, Volume 49, Special Issue D (pp. 41-48) 2017

Activated carbon from waste biomass as host matrix of binary copper and manganese oxide catalysts for methanol decomposition

T. S. Tsoncheva[1]*, G. S. Issa[1], R. N. Ivanova[1], M. D. Dimitrov[1], I. P. Spassova[2], D. G. Kovatcheva[2], B. G. Tsyntsarski[1], N. V. Petrov[1]

[1] *Institute of Organic Chemistry with Centre of Phytochemistry, Bulgarian Academy of Sciences, 1113 Sofia, Bulgaria,*
[2] *Institute of General and Inorganic Chemistry, Bulgarian Academy of Sciences, 1113 Sofia, Bulgaria*

Received, 11 April 2017; Revised, 25 April 2017

Dedicated to Acad. Ivan Juchnovski on the occasion of his 80th birthday

Agriculture wastes, such as peach and apricot stones and grape seeds, were used for the preparation of high quality activated carbons. Thus obtained carbon materials were modified by incipient wetness impregnation with methanol solution of copper and manganese nitrates in different proportion, followed by precursor decomposition in nitrogen. The parent and modified materials were characterized by different physicochemical techniques such as XRD, Nitrogen physisorption, FTIR, UV-Vis, TPR with hydrogen and Boehm method. The catalytic properties of the obtained composites were tested in methanol decomposition with a potential as hydrogen carrier. It was demonstrated that the carbon host matrix promoted the formation of complex mixture of copper and manganese species in different oxidative states. The proportion of various components and the related with them catalytic activity could be easily controlled by Cu/Mn ratio as well as by the texture and surface properties of the activated carbon support, the latter being easily tuned by the agriculture waste precursor used.

Key words: activated carbons from biomass; copper-manganese modifications; methanol decomposition

INTRODUCTION

Nowadays, the greenhouse effect and the ozone layer depletion have considered as the main risks from the transport, industrial and human activity and they demand strong monitoring and control of air emissions [1 and refs therein]. Nevertheless the increasing need of energy and the fluctuation in the energy prices provides the development of new generation of energy devices, such as fuel cells, that are efficient and have minimal environmental impact [2]. Methanol is considered as the most attractive source and carrier of hydrogen for fuel cells supply due to its 5-7 times higher energy density than compressed hydrogen, low sulfur content and availability. It can be produced from variety sources including fossil fuels, agriculture and municipal waste as well as by recycling of carbon dioxide [3-6]. Methanol decomposition has been demonstrated as one of the simplest procedures for hydrogen release but the synthesis of low cost and effective catalysts is still a matter of challenge, especially in case of the application for portable and mobile fuel processors [7]. Copper manganese spinel oxides have been found to be superior catalysts for number of catalytic reactions, including methanol steam reforming [8-10 and ref. therein]. Morales et al. [11] considered that small quantity of copper prevented manganese oxide crystallization, while segregation of CuO was detected in the excess of copper. The high activity of $Cu_xMn_{3-x}O_4$ phase was generally attributed to the presence of two Jahn-Teller ions, Mn^{3+} and Cu^{2+}. The solid state redox exchange between them provides the existence of copper and manganese ions in different oxidative state [2]. In our previous study we demonstrated that activated carbon could be suitable host matrix for the stabilization of transition metal particles in the nanoscale due to its high surface area and well developed porous structure [12-14]. The most attractive feature of the activated carbons (AC) is related to the decrease of their price using renewable and inexpensive sources such as biomass and industrial wastes [15]. We demonstrated that the active phase in monocomponent copper [16] and manganese [17] AC modifications represents a complex mixture of metal and/or metal oxides due to the reduction activity of carbon support during the preparation procedure. Nevertheless the state of manganese on activated carbon has been a question of intensive debates in the literature [18], and to the best of our knowledge, no data for the effect of AC on the formation of binary copper and manganese oxides has been published yet. This investigation is aimed

* To whom all correspondence should be sent:
E-mail: *tsoncheva@orgchm.bas.bg*

at the application of AC from different agriculture residues, such as peach and apricot stones and grape seeds, as catalyst support for $Cu_xMn_{3-x}O_4$ (x=1 or 2) binary oxides for methanol decomposition. The effect of AC texture and surface characteristics on the formation of active phase was in the focus of the investigation. KIT-6 mesoporous silica was used as reference support.

EXPERIMENTAL

Materials

Apricot stones and grape seeds based activated carbons, denoted as ACA and ACG, respectively, were produced by hydropyrolysis at 1023 K for 1 h. This is a one step process involving pyrolysis of the precursor in the presence of steam and activation at the final temperature. Peach stones based activated carbon, denoted as ACP was produced by two-step process, including carbonization at 823 K for 1 h and subsequent activation of the carbonizate with water vapor at 1123 K for 45 min. Mesoporous silica KIT-6 was obtained by procedure described in [19]. The ACs and KIT-6 were modified with copper and manganese (Cu/Mn=1 or 2 mol ratio) by incipient wetness impregnation with methanol solution of the corresponding nitrate precursors. The nitrates decomposition was carried out in a flow of N_2 at 773 K for 2 h (5 K/min). Metal loading in all samples was 8 wt%. The samples were denoted as xCu(3-x)Mn/S, where x was 1 or 2 mol ratio and S was the ACP, ACA, ACG or KIT-6 support.

Methods of characterization

The texture characteristics were determined by N_2 physisorption at 77 K by a Quantachrome NOVA 1200 apparatus. The N_2 adsorption–desorption isotherms were analyzed to evaluate the following parameters: specific surface areas (S_{BET}) was determined on the basis of BET equation; total pore volume (V_t) was estimated in accordance with the Gurvich rule at a relative pressure close to 0.99. The amount of various acidic oxygen-containing functional groups was determined by Boehm's method using aqueous solutions of $NaHCO_3$, Na_2CO_3, NaOH, and C_2H_5ONa [21]. The amount of basic sites was determined with 0.05 N HCl [22]. The pH values were determined after boiling for 5 min in 100 ml H_2O, decantation and cooling of the solution to ambient temperature. Powder X-ray diffraction patterns were collected within the range of 5.3 to 80° on a Bruker D8 Advance diffractometer with Cu K_α radiation and LynxEye detector. Mean crystallite size were determined by the Topas-4.2 software package using the fundamental parameters peak shape description including appropriate corrections for the instrumental broadening and diffractometer geometry. The UV–Vis spectra were recorded using a Jasco V-650 spectrophotometer, equipped with a diffuse reflectance unit. The FTIR spectra (KBr pellets) were recorded on a Bruker Vector 22 spectrometer with resolution 1 cm^{-1} using 64 scans. The TPR/TG (temperature-programmed reduction/thermo-gravimetric) analysis was performed with a Setaram TG92 instrument in a flow of 50 vol% H_2 in Ar (100 cm^3 min^{-1}) and heating rate of 5 K min^{-1}.

Catalytic tests

The catalytic tests were carried out in a flow type fixed bed reactor (0.055 g of catalyst). Methanol (1.57 kPa) was introduced into the reactor from a saturator, thermostated at 273 K using argon as a carrier gas (50 cm^3 min^{-1}). The catalysts were tested under conditions of a temperature-programmed regime within the range of 350–770 K with heating rate of 1 K min^{-1}. Before the catalytic test the samples were treated under Ar flow at 373 K for 1 h and methanol amount was registered using by-pass of the reactor. On-line gas chromatographic analyses were performed on HP apparatus equipped with flame ionization and thermo-conductivity detectors, on a PLOT Q column. Absolute calibration method and a carbon based material balance were used for the calculation of methanol conversion and the yields of various products. The product selectivity at selected temperature was calculated as Y*i*/X*100, where Y*i* was the yield of the *i* product (calculated as detected amount of *i* product/initial amount of methanol, before the introduction in the catalytic reactor) and X was the methanol conversion at this temperature.

RESULTS AND DISCUSSION

The temperature dependencies of methanol decomposition at 550-750 K (Fig. 1a) and the conversion at the final temperature (750 K) for various copper and manganese modifications are presented in Fig. 1. The carbon based materials exhibited catalytic activity just above 650-700 K, while it was registered at about 80-120 K lower temperature for their KIT-6 analogues (Fig. 1a).

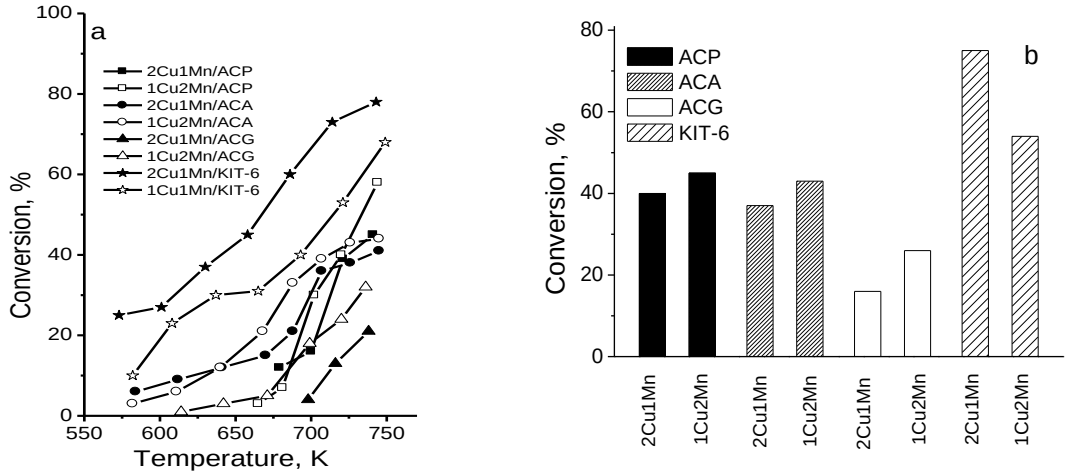

Fig. 1. Temperature dependencies of methanol decomposition (a) and conversion at 750 K (b) for various copper and manganese modifications.

The selectivity to CO, which formation is strongly related to the ability of the samples to release hydrogen from methanol, represented about 80 % at 750 K. Methane and CO_2 were also detected as by-products.On the base of the shift of the conversion curves with the temperature (Fig.1a) and the conversion achieved at the final temperature (Fig. 1b) the samples with given composition $Cu_xMn_{(3-x)}O_4$ (x=1 or 2) could be arranged as follows: xCu(3-x)Mn/KIT-6 > xCu(3-x)Mn/ACP > xCu(3-x)Mn/ACA > xCu(3-x)Mn/ACG. A well defined tendency for a decrease in the catalytic activity with copper content increase was observed for all carbon modifications. Note that this trend was the opposite for the silica based materials. Obviously, a strong effect of the support on the formation of the catalytic active phase could be expected. In order to understand this in detail, complex characterization of the samples by different physicochemical techniques was carried out.

Nitrogen physisorption isotherms (not shown) for the parent and modified activated carbons and KIT-6 were analyzed and the obtained characteristics are listed in Table 1. The parent AC materials characterized with mixed micro-mesoporous texture which ensured significantly high BET surface area. According to the increase in the BET surface area, pore volume and the relative part of mesopores (V_{mes}/V_{mic}) the carbon supports arranged in the following order ACG < ACA < ACP, which is similar to the increase in the catalytic activity of their modifications (see section 3.1). Note that the modification procedure decreased the BET surface area and pore volume and these effects were more pronounced for the ACP and ACA based samples. This could be attributed to pore blocking due to the deposition of metal containing particles in them. The observed change in the V_{mes}/V_{mic} ratio after the modification suggests predominant location of metal species in the mesopores of ACP, while blocking of micropores in higher extent could be assumed for ACA. The significant increase in the V_{mes}/V_{mic} ratio combined with negligible and even absence of changes in the BET surface area for ACG modifications (Table 1) do not exclude structure collapse with the carbon support during the modification procedure as well as deposition of metal particles on the external surface. KIT-6 represented similar BET surface area and more than twice higher pore volume as compared to ACA due to the presence of high amount of mesopores. The decrease in the BET surface area and pore volume and the slight changes in the V_{mes}/V_{mic} ratio reveal almost random distribution of metal particles into the micro- and mesopores of the silica support. Taking into account the highest activity of KIT-6 modifications (Fig. 1) one could be assumed that the texture characteristics of the support seem to be important, but not the dominant factor for the formation of active phase.

FTIR spectra of parent and modified activated carbons are presented in Fig. 2. The bands at around 3028 cm^{-1} were attributed to C-H stretching vibrations in CH_3 groups. The band at about 1715 cm^{-1} corresponded to C=O stretching vibrations in lactonic, carbonyl or anhydride groups. The bands at 1535 and 1036 cm^{-1} were assigned to ring vibration in aromatic skeleton, typical of carbon materials [23].

Table 1. Nitrogen physisorption data for parent and modified activated carbons and KIT-6 materials: (S_{BET}-BET surface area, S_{mi}- surface area of micropores, V_t-total pore volume, V_{mi}-micropores pore volume, D_{av}-average pore diameter).

Sample	SBET, m2/g	Smi, m2/g	Vt, cm3/g	Vmi cm3/g	Dav nm	ΔS %	ΔV %	Vmes/ Vmic
ACP	1258	1116	0.61	0.45	1.94			0.35
2Cu1Mn/ACP	1006	956	0.49	0.40	1.97	20	20	0.22
1Cu2Mn/ACP	1080	1024	0.53	0.43	1.97	14	13	0.23
ACA	921	874	0.46	0.37	2.0			0.24
2Cu1Mn/ACA	743	625	0.38	0.28	2.0	19	17	0.36
1Cu2Mn/ACA	794	676	0.39	0.28	1.9	14	15	0.39
ACG	603	577	0.28	0.24	1.9			0.17
2Cu1Mn/ACG	603	522	0.25	0.18	2.0	0	10	0.39
1Cu2Mn/ACG	548	456	0.26	0.17	1.9	9	7	0.53
KIT-6	872	278	1.23	0.14	8.1			7.78
2Cu1Mn/KIT-6	748	220	1.09	0.11	5.8	14	11	8.91
1Cu2Mn/KIT-6	722	189	1.05	0.09	5.8	17	18	10.67

The band at c.a. 1094 cm^{-1} could be due to vibrations in ether C-O-C groups. The broad band in the 800-600 cm^{-1} region could be assigned to C=C bending vibrations in aromatic and non-aromatic structures. The change in the intensity and the position of the FTIR bands after the AC modification (Fig.2b) revealed interaction of metal species both with the surface functional groups and carbon basal planes. The additional bands in the 700-400 cm^{-1} region for the modified materials could be due to Mn-O and Cu-O vibrations in different coordination and oxidative state of the metal ion [24, 25]. More precise characterization of surface functional groups of AC was carried out by Boehm method [21] and titration with HCl [22] and the data are shown in Table 2. Presence of surface hydroxyl and carbonyl acidic groups as well as basic functional groups was detected for all activated carbons. Their amount was lowest for ACP, followed by ACG and ACA. The pH values and the relatively low acidic/basic groups ratio for ACP indicated higher basicity which was provoked by the presence of relatively high amount of surface basic groups.

XRD patterns of parent and modified carbon and silica supports are presented in Fig. 3 and data for the phase composition, unit cell parameters and average crystallite size are listed in Table 3. XRD patterns of activated carbons represented reflections at 2θ= 25-26° and 45° which could be assigned to carbon turbostratic structure [15]. The reflections were narrower for ACP and ACA indicating relatively high carbon crystallinity. Just the opposite, the broader reflections for ACG evidenced presence of amorphous carbon phase. The additional narrow reflections at 2θ=43.4°, 50.8° and 74.4°, which appeared in the XRD patterns of all carbon based modifications could be ascribed to (111), (200) and (220) planes respectively of face centered cubic metallic copper (pdf 85-1326). The average particles size varied in the 20-50 nm range. The reflections became more intensive for the samples with higher copper content (2Cu1Mn/AC) which was in accordance with the data reported in the literature [2]. In addition, slight reflections at 2θ= 29.5°, 36.2°, 42.5°, 61.4° and 73.4° corresponding to (110), (111), (200), (220) and (311) planes of Cu_2O (primitive cubic Pn-3m, pdf 071- 3645) with average particle size of 3-20 nm (Table 3) were observed.

Table 2. Data for the pH and surface acidic and basic groups for the activated carbon supports.

sample	pH	acidic surface functional groups				basic groups
		carb.	lact.	hydr.	carb.	
ACP	9.4	BDL	BDL*	0.29	1.07	1.04
ACA	8.7	BDL	BDL	2.05	3.27	1.34
ACG	8.9	BDL	BDL	1.59	2.98	1.24

*BDL-bellow detection limit

Single manganese phases such as MnO (pdf 075-1090) and Mn_3O_4 (pdf 080-0382) were detected for both ACG based materials and 1Cu2Mn/ACA, respectively. Single manganese phases such as MnO (pdf 075-1090) and Mn_3O_4 (pdf 080-0382) were detected for both ACG based materials and 1Cu2Mn/ACA, respectively.

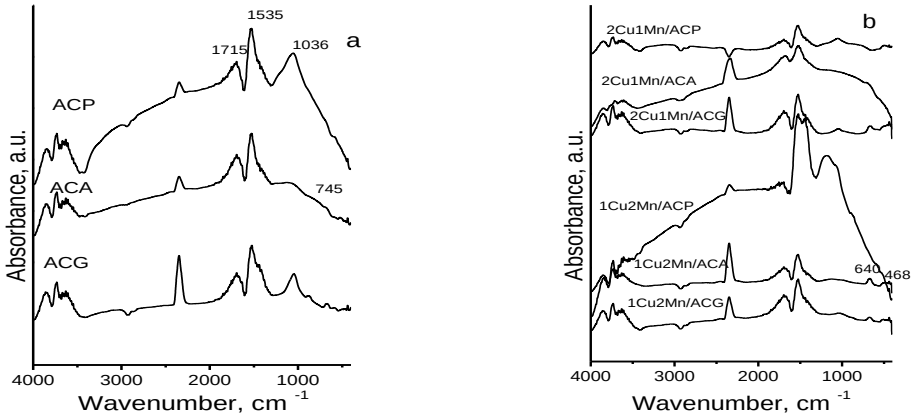

Fig 2. FTIR spectra of parent activated carbons (a) and their copper-manganese modifications (b).

The appearance of well defined, but low intensive reflections at 2θ=36.6º, 44º and 58º in the patterns of both ACP modifications and 1Cu2Mn/ACA indicated formation of small amount of finely dispersed face centered cubic Fd-3m non-stoihiometric $Cu_{1.5}Mn_{1.5}O_4$ spinel phase (pdf 070-0262).Thus, carbon support renders difficult the formation of spinel copper-manganese phase. Due to the reduction activity it readily provokes the segregation of reduced copper (Cu, Cu_2O) and manganese (MnO, Mn_3O_4) phases during the metal precursor decomposition. This effect seems to be slightly suppressed for ACP. Taking into account the texture and surface characterization of AC supports (see above) can be concluded that the low concentration of surface functional groups and the better developed mesoporous structure of activated carbon provoke the stabilization and intimate contact between highly dispersed metal oxide entities and facilitate the formation of binary oxides. The assumption for the role of A C support on the formation of copper-manganese phase was confirmed by the reference KIT-6 based samples (Table3, Fig.3). Here absence (1Cu2Mn/KIT-6) or slight (2Cu1Mn/KIT-6) reflections of face-centered cubic Fd-3m $Cu_{1.4}Mn_{1.6}O_4$ phase (pdf 071-1145) were observed indicating that the inert mesoporous matrix promoted the formation of highly dispersed spinel mixed oxide. UV-Vis spectra of selected carbon materials (ACG) and reference KIT-6 based samples are presented in Fig.4. The intense absorption feature at ca. 325 nm in the spectra of the latter materials could due to the excitation of surface plasmon in the spinel, in consistence with the XRD data (Fig. 3, Table 3). The additional absorption peak at 688 nm in the spectrum of 2Cu1Mn/KIT6 could be due to the segregation of the excess of CuO in the sample with high Cu/Mn ratio [2]. At the same time, the absorption in the visible region of UV-Vis spectrum of Mn/ACG falls down

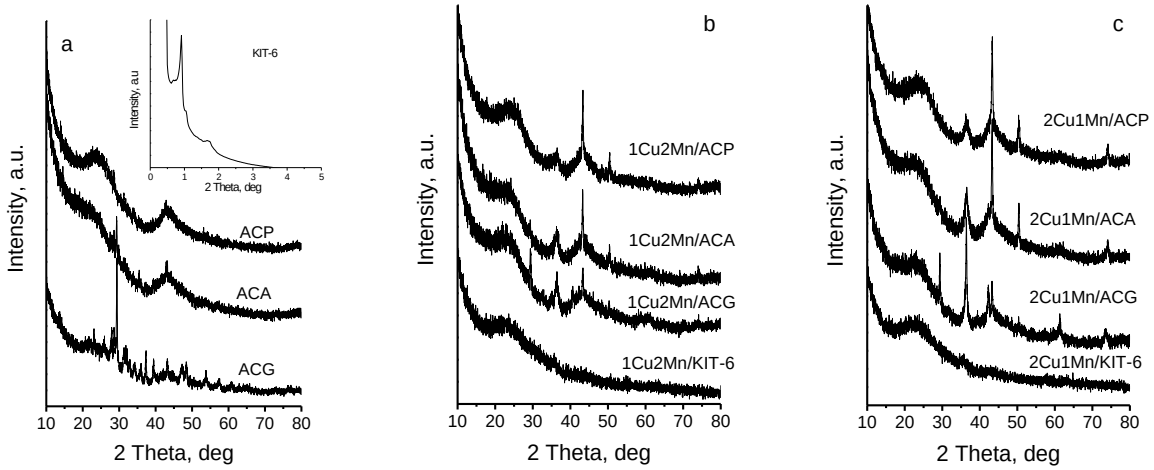

Fig 3. XRD patterns of parent activated carbons (a) and KIT-6 (a,inset) and their 1Cu2Mn/S (b) and 2Cu1Mn/S (c) modifications.

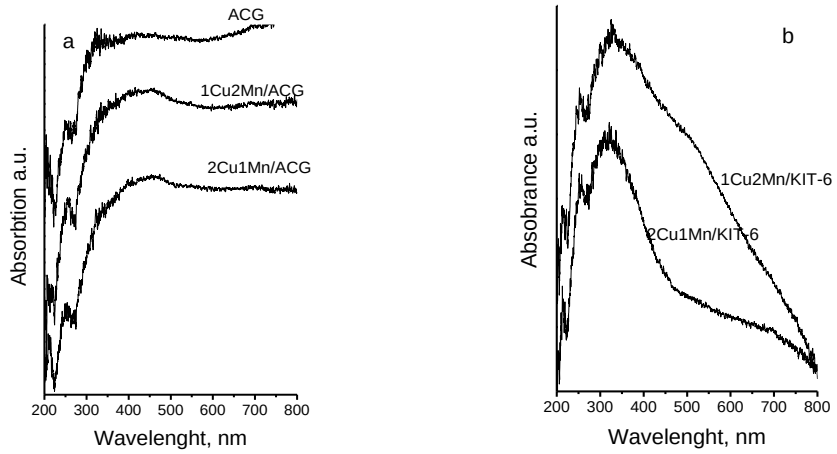

Fig. 4. UV-Vis spectra of ACG (a) and KIT-6 (b) modifications.

This could be due to the non-allowed d-d crystal field transitions of Mn^{2+} ion, which dominated in this sample, in consistence with the XRD analysis [26]. The peaks at 320, 470 and 730 nm could be assigned to $O^{2-} \rightarrow Mn^{3+}$ charge transfer and d-d crystal field transitions in octahedral Mn^{3+} species in hausmannite (Mn_3O_4) phase [26].

In order to characterize the state of copper-manganese active phase more precisely under the conditions that are close to the catalytic experiment, the samples were studied by temperature-programmed reduction with hydrogen. The TPR-TG profiles for carbon and KIT-6 modifications are presented in Fig. 5.

Table 3. Phase composition, unit cell parameters and average crystalline size for various copper-manganese modifications

Sample	Phase composition	Unit cell, Å	Particles size, nm
1Cu2Mn/A	Cu^0	.62	50
CP	Cu_2O	4.28	3
	$Cu_{1.5}Mn_{1.5}O_4$	8.290	
1Cu2Mn/A	Cu^0	3.62	27
CA	Cu_2O	4.28	7
	Mn_3O_4	a=5.765	
		c=9.442	
	$Cu_{1.5}Mn_{1.5}O_4$	8.290	
1Cu2Mn/A	Cu0	3.62	43
CG	Cu2O	4.268	10
	MnO	4.446	
1Cu2Mn/ KIT-6	amorphous		
2Cu1Mn/A	Cu0	3.620(1)	24
CP	Cu2O	4.287(3)	6
	Cu1.5Mn1.5O4	8.290	
2Cu1Mn/A	Cu0	3.616(1)	40
CA	Cu2O	4.269(2)	8
2Cu1Mn/A	Cu0	3.619(1)	20
CG	Cu2O	4.275(1)	25
	MnO	4.446	
2Cu1Mn/ KIT-6	Cu1.4Mn1.6O4	8.30	

The main TPR effects for reference 1Cu2Mn/KIT-6 and 2Cu1Mn/KIT-6 modifications were centered at 535 and 460 K, respectively, which according to the XRD and UV-Vis spectra, could be assigned to the reduction of spinel like $Cu_xMn_{3-x}O_4$ particles. These features are shifted to lower temperatures in comparison with the reported in the literature data for the Mn_xO_y reduction which confirms the facilitated effect of copper addition [2 and refs therein]. The shift of the main TPR effect for the Cu-rich modification to lower temperature (Fig. 5) could be due to the reduction of segregated excess of CuO, which was in consistence with the UV-Vis data (Fig.4). The main reduction effect in the TPR-profiles of AC based binary modifications was broader, less intensive and temperature shifted as compared to their reference analogues. In accordance with the XRD data (Table 3, Fig. 3) it could be due to the superposition of the reduction effects for a mixture of spinel phase and partially reduced copper and manganese oxides (Cu_2O, Mn_3O_4) in different proportion (Table 3). Thus, the extremely low reduction effect for 1Cu2Mn/ACG could be related to domination of metallic Cu and MnO in it (Table 3). In contrast to the silica based samples, strong effect of weight loss above 650 K was also observed for all AC modifications. It overcame the expected weight loss for the reduction of the loaded active phase, which indicates changes with the carbon support under the reduction medium. So, we can expect that under the reduction reaction medium during the methanol decomposition spinel oxides decompose with the formation of metallic Cu and MnO [27]. Although the mechanism of methanol decomposition on copper containing catalysts has been widely studied, the interaction of copper with second metal oxide makes the prediction of its behaviour rather complicated [28].

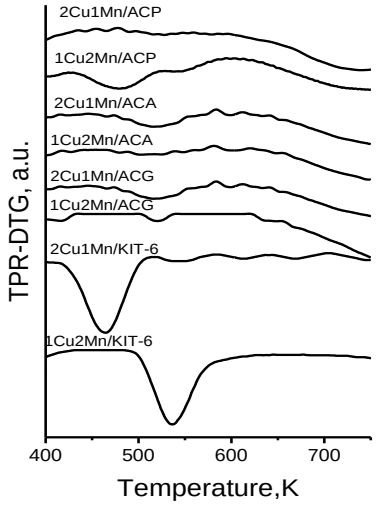

Fig 5. TPR-DTG profiles of AC and KIT-6 odifications

Restoration of OH groups on metal oxide by spillover of hydrogen from copper was proposed for the increase formation of surface intermediate methoxy groups by Bianchi et al. [29], Fisher and Bell [30] assumed reverse spillover of hydrogen from metal oxide to Cu, while Manzoli [31] suggested change in the oxygen vacancy equilibrium between Cu and metal oxide as more appropriate reason for the synergistic effect between them. Nevertheless the type of realized mechanism the dispersion of various metal oxide particles and the close contact between them should be of primary importance for the formation of spinel phase. Obviously the ordered mesoporous structure of silica support facilitates the formation of highly dispersed spinel oxide phase or a mixture of spinel and CuO in the excess of copper (Figs. 3,5, Table 3). Moreover, the stabilization of spinel particles in the ordered mesopores suppresses the aggregation of metallic copper particles, formed during the catalytic process, facilitates the intimate contact with the manganese oxide and maintains the accessibility of the reactant particles to the active sites. This provides high catalytic activity in methanol decomposition which increases with the increase of copper content in the samples (Fig. 1). The XRD, UV-Vis and TPR results clearly demonstrate that this is strongly suppressed on the carbon support. Here, due to the reduction ability of AC, metallic copper aggregates and reduced manganese oxide species are formed even during the modification procedure, which renders difficult the formation of active spinel phase and this is more pronounced with the increase of copper content (Fig. 1). The nitrogen physisorption data (section 3.2.1) and surface analyses (section 3.2.2) clearly indicate that the texture characteristics and surface functionality of AC regulate the type and proportion between different copper-manganese species. It seems that the relatively small amount of surface acidic groups (Table 2) and higher mesoporosity (Table 1) of ACP promotes the stabilization of more finely dispersed and highly active spinel species. Just the opposite, the relatively high surface functionality (Table 2) and predominantly microprous structure of ACG (Table 1) suppress the formation of spinel phase due to the facile segregation of metallic Cu and MnO phases (Table 3, Figs. 3,5)

CONCLUSION

Activated carbon from different agriculture residues could be suitable support for copper-manganese catalysts for methanol decomposition. It provokes formation of complex mixture of metallic copper, Cu_2O, MnOx and spinel $Cu_xMn_{3-x}O_4$ particles in different proportion. The lower surface functionality and higher degree of mesoporosity of activated carbon, which can be readily tuned by the agriculture precursor used, as well as the lower Cu/Mn ratio promote the formation of more active catalysts for methanol decomposition.

Acknowledgements: *Financial support project DFNI E02/2/2014 is gratefully acknowledged.*

REFERENCES

1. G. A. El-Shobaky, H. G. El-Shobaky, A. A. Badawy, Y. M. Fahmy, *Applied Catalysis A: General*, **409–410,** 234 (2011).
2. J. Papavasiliou, G. Avgouropoulos, T. Ioannides, *J. Catal*., **251**, 7 (2007).
3. G. Avgouropoulos, T. Ioannides, J. K. Kallitsis, S. Neophytides, *Chem. Eng. J*., **176-177**, 95 (2011).
4. S. Patel, K. K.Pant, *Appl. Catal. A: General*, **356,** 189 (2009).
5. H. Muroyama, R. Nakase, T. Matsui, K. Eguchi, *Int. J. Hydrogen Energy*, **35,** 1575 (2010).
6. R. M. Navarro, M. A. Pena, J. L. G. Fierro, *Chem. Rev*, **107,** 395 (2007).
7. J. Papavasiliou, G. Avgouropoulos, T. Ioannides, *Int. J. Hydrogen Energy*, **37**, 16739 (2012).
8. S. Behar, P. Gonzalez, P. Agulhon, F. Quignard, D. Swierczynski, *Catal. Today*, **189,** 35 (2012).
9. V. H. Vu, J. Belkouch, A. Ould-Dris, B. Taouk, *J. Hazardous Mater*., **169,** 758 (2009).
10. D. A. Aguilera, A. Perez, R. Molina, S. Moreno, *Appl. Catal. B: Environmental*, **104,** 144 (2011).

11. M. R. Morales, B. P. Barbero, L. E. Cadús, *Fuel*, **87,** 1177 (2008).
12. T. Tsoncheva, I. Genova, D. Paneva, M. Dimitrov, B. Tsyntsarski, N. Velinov, R. Ivanova, G. Issa, D. Kovacheva, T. Budinova, I. Mitov, N. Petrov, *Solid State Sci*., **48**, 286 (2015).
13. B. Tsyntsarski, I. Stoycheva, T. Tsoncheva, I. Genova, M. Dimitrov, B. Petrova, D. Paneva, Z. Cherkezova-Zheleva, T. Budinova, H. Kolev, A. Gomis-Berenguer, C.O. Ania, I. Mitov, N. Petrov, *Fuel Process.Technol*., **137**, 139 (2015).
14. T. Tsoncheva, A. Mileva, D. Paneva, D. Kovacheva, I. Spassova, D. Nihtianova, P. Markov, N. Petrov, I. Mitov, *Micropor. Mesopor. Mater*., **229**, 59 (2016).
15. K.-W. Jung, B. H. Choi, M.-J. Hwang, T.-U. Jeong, K.-H. Ahn, *Bioresource Technol*., **219,** 185 (2016).
16. T. Tsoncheva, I. Genova, I. Stoycheva, I. Spassova, R. Ivanova, B. Tsyntsarski, G. Issa, D. Kovacheva, N. Petrov, *J. Porous Mater*., **22,** 1127 (2015).
17. I. Stoycheva, T. Tsoncheva, B. Tsyntsarski, I. Genova, R. Ivanova, B. Petrova, I. Spassova, G. Issa, T. Budinova, N. Petrov, Procc. SGEM 2015 GeoConference of Energy and Clean Technol., 393 (2015).
18. Q. Tang, X. Huang, Y. Chen, T. Liuc, Y. Yang, *J. Mol. Catal. A: Chemical*, **301**, 24 (2009).
19. T. Tsoncheva, I. Genova, M. Stoyanova, M. Pohl, R.Nickolov, M. Dimitrov, E. Priboczki, M. Mihaylov, D.Kovacheva, K.Hadjiivanov, *Appl. Catal. B: Env.*, **147**, 684 (2014).
20. H. P. Boehm, *Adv. Catal. Related Subjects*, **16,** 179 (1966)
21. E. Papier, S. Li, J. B. Donnet, *Carbon*, **25,** 243 (1987).
22. R. C. Sun, J. Tomkinson, *Sep. Purif.Technol.*, **24** 529 (2001).
23. Y. U. Lin, S. U. N. Ming, Y. U. Jian, Y. U. Qian, H.A.O. Zhifeng, L.I. C. Chin, *J. Catal*., **29**, 1127 (2008).
24. Y. C. Zhang, J. Y.Tang, G. L.Wang, M. Zhang, X.Y. Hu, *J. Cryst. Growth*, **294**, 278 (2006).
25. J. B. Macstre, E. F.Lorez, J. M. Gallardo-Amores, R. R. Casero, V. S. Escribano, E. P. Bernal, *Int. J. Inorg. Chem*., **3**, 889 (2001).
26. M. R. Morales, B. P. Barbero, L. E. Cadurs, *Fuel*, **87**, 1177 (2008).
27. S.T. Yong, K. Hidajat, S. Kawi, *Catal. Today*, **131**, 188 (2008).
28. D. Bianchi, T. Chafik, M. Khalfallah, S. J. Teichner, *Appl. Catal. A*:*General*, **123,** 89 (1995).
29. I. A. Fisher, A. T. Bell, *J. Catal.*, **184,** 357 (1999).
30. M. Manzoli, A. Chiorino, F. Boccuzzi, *Appl. Catal. B: Environmental*, **57,** 201 (2005).

АКТИВЕН ВЪГЛЕН, ПОЛУЧЕН ОТ ОТПАДНА БИОМАСА, КАТО НОСИТЕЛ НА СМЕСЕНИ МЕД-МАНГАНОВИ ОКСИДНИ КАТАЛИЗАТОРИ ЗА РАЗЛАГАНЕ НА МЕТАНОЛ

Т. С. Цончева[1]*, Г. С. Исса[1], Р. Н. Иванова[1], М. Д. Димитров[1], И. П. Спасова[2], Д. Г. Ковачева[2], Б. Г. Цинцарски[1], Н. В. Петров[1]

[1] Институт по органична химия с Център по фитохимия, Българска академия на науките, 1113 София, България,

[2] Институт по обща и неорганична химия, Българска академия на науките, 1113 София, България

Постъпила на 11 април 2017 г.; Коригирана на 25 април 2017 г

(Резюме)

Получен е висококачествен активен въглен от различни селскостопански отпадъци, като костилки от праскови и кайсии и семки от грозде. Въглеродните материали бяха модифицирани чрез омокряне с метанолов разтвор на меден и манганов нитрат в различни съотношения и следващо разлагане на прекурсорите в азот. Изходните и модифицирани въглеродни материали бяха характеризирани с различни физикохимични техники като рентгеноструктурен анализ, УВ, ФТИР, ТПР с водород и метод на Бьом. Каталитичните свойства на получените композити бяха изпитани в разлагане на метанол, с потенциално приложение като източник и преносител на водород. Показано е, че въглеродният носител благоприятства формирането на сложна смес от медни и манганови частици в различно окислително състояние. Съотношението между различните компоненти и свързаната с тях каталитична активност може лесно да се контролира чрез отношението Cu/Mn, както и посредством текстурните и повърхностни свойства на активния въглен, като последните могат лесно да се променят чрез използвания селскостопански отпадък.